

Inhibition of a SNARE-Sensitive Pathway in Astrocytes Attenuates Damage following Stroke

Dustin J. Hines and Philip G. Haydon

Department of Neuroscience, Tufts University School of Medicine, Boston, Massachusetts 02111

A strong body of research has defined the role of excitotoxic glutamate in animal models of brain ischemia and stroke; however, clinical trials of glutamate receptor antagonists have demonstrated their limited capacity to prevent brain damage following ischemia. We propose that astrocyte–neuron signaling represents an important modulatory target that may be useful in mediating damage following stroke. To assess the impact of astrocyte signaling on damage following stroke, we have used the astrocyte-specific dominant-negative SNARE mouse model (dnSNARE). Recent findings have shown that the astrocytic SNARE signaling pathway can affect neuronal excitability by regulating the surface expression of NMDA receptors. Using focal photothrombosis via the Rose Bengal method, as well as excitotoxic NMDA lesions, we show that dnSNARE animals exhibited a sparing of damaged tissue quantified using Nissl and NeuN staining. At the same time point, animals were also tested in behavioral tasks that probe the functional integrity of stroke- or lesion-damaged motor and somatosensory areas. We found that dnSNARE mice performed significantly better than littermate controls on rung walk and adhesive dot removal tasks following lesion. Together, our results demonstrate the important role of astrocytic signaling under ischemic conditions. Drugs targeting astrocyte signaling have a potential benefit for the outcome of stroke in human patients by limiting the spread of damage.

Introduction

The pathophysiology of neuronal damage caused by ischemic injury has been extensively studied; however, most studies have focused solely on neuronal mechanisms (Barreto et al., 2011a). Ischemia is a serious condition in which the cerebral blood supply within the brain is restricted, typically by thrombotic and/or embolic events. Severe ischemia causes acute neuronal death within minutes in the ischemic core (infarct), whereas secondary, expanding neuronal death occurs in the penumbra (or perinfarct) within hours (Ginsberg and Pulsinelli, 1994; Hossmann, 1994). Several mechanisms contribute to the extent of damage, including glutamate and Ca²⁺ toxicity, oxidative stress, inflammation, mitochondrial dysfunction, and acidosis (Barber et al., 2003; Mattiasson et al., 2003; Xiong et al., 2004; Eltzschig and Eckle, 2011). Extensive research has focused on glutamate-mediated excitotoxicity in animal models of brain ischemia and stroke. However, clinical trials of glutamate receptor antagonists have demonstrated their limited capacity to prevent brain damage following human ischemia (Ikonomidou and Turski, 2002; Hoyte et al., 2004; Lipton, 2004; Muir, 2006). The lack of positive results from these approaches may relate to the fundamental role of neuronal glutamate in brain signaling (Ikonomidou and Tur-

ski, 2002), and indeed failure of many approaches used to prevent damage following stroke could be due to the exclusive focus on neuronal function.

Astrocytes are the predominant glial cell type in the CNS that modulates neuronal function, although there is little insight into how they might impact the consequences of ischemia (Barreto et al., 2011b). Astrocytes are well known to maintain structural integrity and to be tightly coupled to neuronal metabolism via the vasculature (Haydon and Carmignoto, 2006; Attwell et al., 2010). Astrocytes not only play supportive roles in brain function but also play an active role in modulating neuronal function. Astrocytes express a variety of receptors, some of which are able to induce the release of chemical transmitters for interaction and communication with neurons (for review, see Haydon, 2001). Astrocytes have been shown to affect neuronal excitability via multiple mechanisms (Oliet et al., 2004; Haydon and Carmignoto, 2006; Zorec et al., 2012). In particular, astrocyte signaling has been shown to regulate the surface expression of NMDA receptors, thereby regulating the NMDA component of synaptic transmission (Deng et al., 2011).

Astrocytes retain their structural integrity for hours following photothrombosis, and exhibit receptor-mediated Ca²⁺ oscillations in the ischemic region, which when selectively buffered can result in protection from damage in a stroke model (Ding et al., 2009). We have used a genetic mouse model that selectively interferes with astrocyte signaling via conditional expression of a dominant-negative SNARE protein under control of the GFAP promoter (dnSNARE) (Halassa et al., 2009) to further probe the role of these glia in stroke. We demonstrate that dnSNARE mice show reduced lesion volume and improved behavioral performance following photothrombosis and show improved histolog-

Received Nov. 28, 2012; accepted Jan. 3, 2013.

Author contributions: D.J.H. and P.G.H. designed research; D.J.H. performed research; D.J.H. contributed unpublished reagents/analytic tools; D.J.H. analyzed data; D.J.H. and P.G.H. wrote the paper.

This work was supported by NIH Grants R01 NS037585, R01 MH095385 to P.G.H., and by grants from The Heart and Stroke Foundation of Canada to D.J.H.

Correspondence should be addressed to Philip G. Haydon, Department of Neuroscience, Tufts University School of Medicine, 136 Harrison Avenue, Boston, MA 02111. E-mail: philip.haydon@tufts.edu.

DOI:10.1523/JNEUROSCI.5495-12.2013

Copyright © 2013 the authors 0270-6474/13/334234-07\$15.00/0

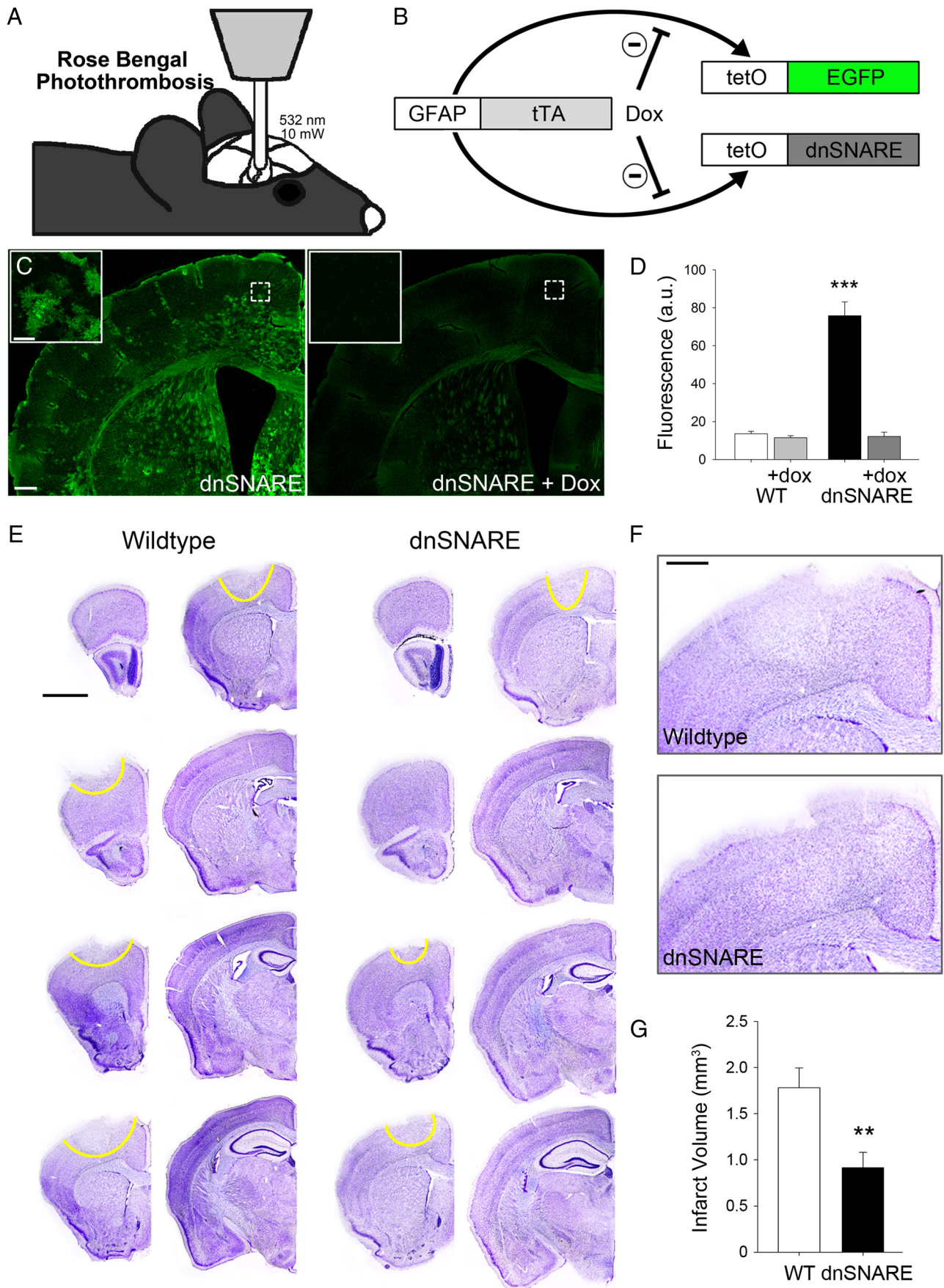


Figure 1. Damage following Rose Bengal photothrombosis is attenuated in mice expressing dnSNARE in astrocytes. *A*, Photothrombosis is achieved via intraperitoneal injection of Rose Bengal and illumination (532 nm, 10 mW) of the sensory-motor cortex through a cranial window. *B*, Astrocyte-selective expression of dnSNARE (and EGFP) via GFAP (Figure legend continues.)

ical outcomes following NMDA lesions. Together, our results demonstrate the important role of astrocytic signaling under ischemic conditions and provide new insights regarding neuron–glia interactions.

Materials and Methods

All procedures were carried out in accordance with the National Institutes of Health *Guide for the Care and Use of Laboratory Animals* and were approved by the Tufts University Institutional Animal Care and Use Committee.

dnSNARE mice

The dnSNARE mouse strain (Pascual et al., 2005) has been previously characterized (Fellin et al., 2009; Halassa et al., 2009). Germ-line transmission of the transgenes was detected using PCR to identify all experimental animals. The dnSNARE mice have been backcrossed onto a C57BL/6J genotype for >10 generations, and littermates were used as controls in all experiments. To allow normal brain development, dnSNARE animals and their littermates were maintained on a diet containing doxycycline, to suppress transgene expression, until weaning (Fellin et al., 2009; Halassa et al., 2009). EGFP reporter expression has previously been shown to occur selectively in astrocytes, as demonstrated using antibodies to GFAP (astrocyte marker) and NeuN (neuronal cell marker) (Fellin et al., 2009; Halassa et al., 2009). All mice used in experiments were males ranging from 12 to 16 weeks of age.

Photothrombosis

Unilateral ischemic strokes were induced in the sensory-motor cortex using the photothrombotic method (Watson et al., 1985; Brown et al., 2010). Mice were anesthetized with ketamine/xylazine (100 mg/kg ketamine and 10 mg/kg xylazine, i.p.), fitted into a stereotaxic frame. To induce stroke, a cranial window was created above the forelimb cortex [anteroposterior (A/P), 0.0; mediolateral (M/L), +1.5] (Tennant et al., 2011), and this region was illuminated with green epifluorescent light for 12 min after an injection of 1% Rose Bengal solution (100 mg/kg, i.p., in PBS).

NMDA lesion

NMDA lesions were based on previously established protocols (Kim et al., 2006). Mice were anesthetized with ketamine/xylazine (100 mg/kg ketamine and 10 mg/kg xylazine, i.p.) and fitted into a stereotaxic frame. A small burr hole was drilled centered on the forelimb area, and 1 μ l of a 10 mg/ml NMDA solution (dissolved in sterile artificial CSF) was injected into the lesion site. In the case of the contralateral lesion, the skull above the area was drilled with a burr hole but no injection was performed.

Histology and immunohistochemistry

Animals were transcardially perfused with a 4% paraformaldehyde solution. Sections 40 μ m thick were cut serially, and a subset was reserved for Nissl staining. Remaining sections were stained free floating with anti-GFP (chicken, Millipore) and anti-NeuN (mouse, Millipore Bioscience Research Reagents), followed by corresponding secondary antibodies (Invitrogen). Images were taken with a 20 \times objective on a Nikon confocal microscope and were quantified using ImageJ.

←

(Figure legend continued.) promoter control of the tetracycline controlled transactivator (tTA) and tetracycline responsive element (tetO) doxycycline-sensitive system. **C**, Representative image of EGFP fluorescence in dnSNARE mice off (left) and on (right) doxycycline chow. **D**, Quantification of EGFP fluorescence in sensory-motor cortex of wild-type and dnSNARE littermates, on and off doxycycline. **E**, Representative images of Nissl-stained sections from a wild-type mouse and a dnSNARE mouse subjected to unilateral photothrombosis. **F**, Zoom comparing matched wild-type and dnSNARE Nissl-stained sections from mice subjected to unilateral photothrombosis. **G**, Quantification of infarct volume calculated from reconstructed serial section sets in wild-type and dnSNARE mice subjected to photothrombosis. Dox, Doxycycline. ** $p < 0.01$, *** $p < 0.001$.

Behavioral assessments

Rung walk. The rung walk assessment was based on methods described by Farr et al. (2006). The rung walk apparatus was composed of two Plexiglas walls (69.5 \times 15 cm). Each wall contained 121 holes, 0.20 cm in diameter, spaced 0.5 cm apart, and located 1 cm from the bottom edge of the wall. The holes could be filled with 8-cm-long metal bars, with a diameter of 0.10 cm. The walls were spaced 5 cm apart to allow for passage of a mouse but to prevent it from turning around. The entire apparatus was placed atop two standard mouse housing cages, 17 cm above the ground. The first tub served as a neutral start location, and the goal tub was the animal's home cage.

Adhesive dot removal. This task was based on methods previously described (Schallert and Whishaw, 1984), and requires mice to detect and remove pieces of adhesive paper from their wrists. The distal-radial aspects of forelimbs were cleaned with 70% alcohol and an adhesive sticker was applied to the limb contralateral to the photothrombotic lesion. We then quantified the latency to sticker removal (average over each of four trials) to assess the ability of the mouse to perform sensorimotor tasks.

Results

Expression of dnSNARE in astrocytes reduces the extent of damage following photothrombosis

Pregnant females and offspring were fed doxycycline-containing chow to suppress the expression of EGFP and dnSNARE until weaning (Fig. 1A–C). Subsequently, mice were separated into two groups, one that was fed normal food and the other that was maintained on a diet containing doxycycline. At 9 weeks of age, the intensity of EGFP expression in both groups of animals was compared. In the absence of doxycycline, the intensity of EGFP fluorescence was 75.8 ± 7.3 a.u. compared with 12.2 ± 2.2 a.u. when doxycycline was maintained in the diet of dnSNARE mice ($p < 0.001$). Doxycycline prevented transgene expression, and thus fluorescence intensity was not different from wild-type littermate control mice (13.6 ± 1.3 a.u.) or wild-type littermate control mice fed doxycycline chow (11.5 ± 1.1 a.u.; Fig. 1D).

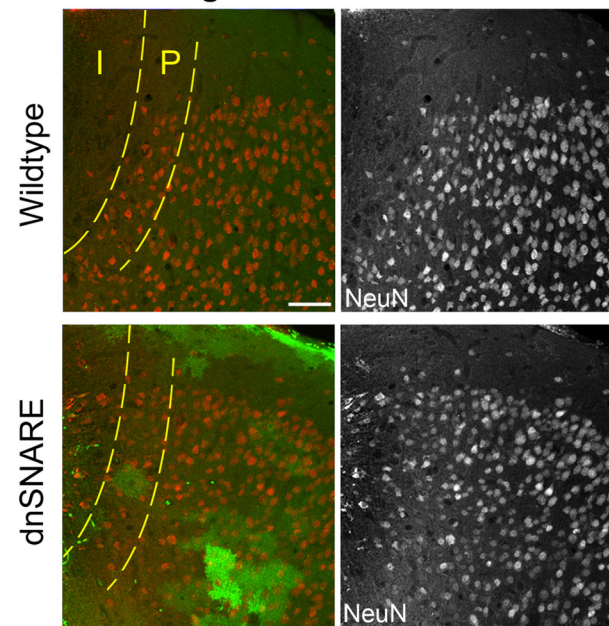
Groups of dnSNARE and matched wild-type littermate controls were subjected to unilateral Rose Bengal photothrombosis using stereotaxic coordinates to generate a cranial window above the forelimb sensory-motor area (A/P, 0.0; M/L, +1.5) (Tennant et al., 2011). At 24 h postlesion, mice were killed by transcardial perfusion and serial tissue sections were cut for analysis of infarct volume with Nissl-stained sections (Fig. 1E, F). Wild-type mice had a mean infarct volume of 1.80 ± 0.22 mm³, which was significantly greater ($p = 0.019$) than mice expressing dnSNARE (0.93 ± 0.17 mm³; Fig. 1G), suggesting that the expression of dnSNARE in astrocytes may aid in tissue sparing in the photothrombosis model of stroke.

Neurons are spared within the photothrombosis infarct and peri-infarct regions in mice expressing dnSNARE

Tissue sections from mice that had undergone unilateral photothrombosis were also processed for immunohistochemistry for the neuronal marker NeuN to allow an assessment of neurons in the infarct and peri-infarct regions (Fig. 2A, B). To examine the number of NeuN-positive cells, we sampled multiple regions, 50 μ m tall by 50 μ m wide and 25 μ m deep ($62,500 \mu$ m³). Within the infarct region, wild-type mice had an average of 1.01 ± 0.37 NeuN-positive neurons per $62,500 \mu$ m³. In contrast, mice expressing dnSNARE had an average of 4.33 ± 1.17 NeuN-positive neurons per $62,500 \mu$ m³ of infarct region, demonstrating that dnSNARE mice had significantly greater numbers of neurons in the infarct region ($p = 0.039$; Fig. 2C).

Assessments of NeuN-positive cells in the peri-infarct region also showed significantly greater numbers in dnSNARE mice

A Rose Bengal Photothrombosis



B Contralateral

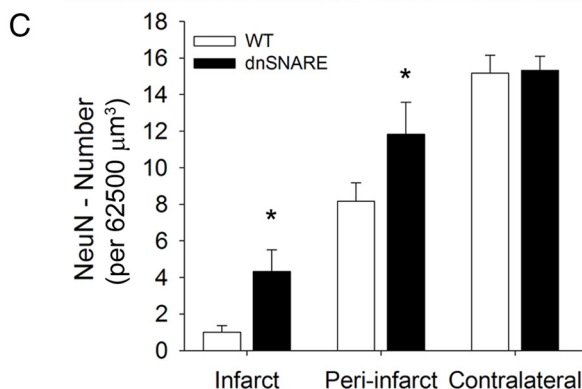
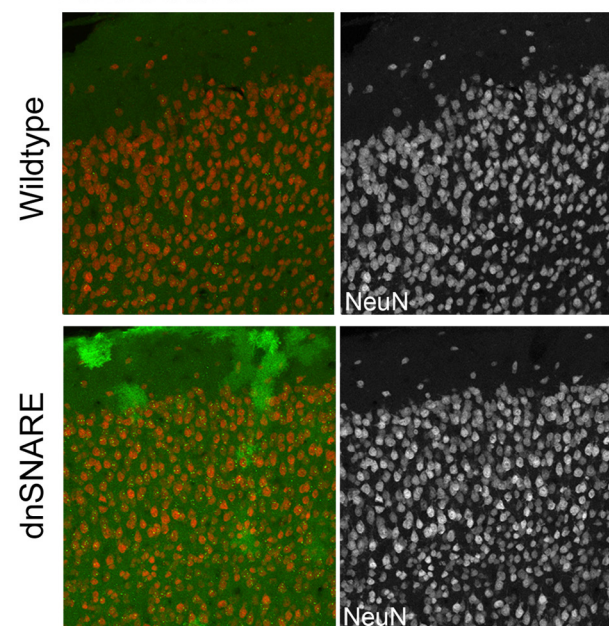


Figure 2. Mice expressing dnSNARE show sparing of neurons in infarct and peri-infarct regions following photothrombosis. **A**, Representative image of NeuN (red) staining in

(11.83 ± 1.74) compared with wild-type mice (8.17 ± 1.01 ; $p = 0.024$; Fig. 2C). No difference was observed in the number of NeuN-positive neurons per $62,500 \mu\text{m}^3$ of contralateral hemisphere sensory-motor cortex between wild-type littermates (15.17 ± 0.98) and dnSNARE (15.33 ± 0.76) mice subjected to photothrombosis (Fig. 2C).

Mice expressing dnSNARE show better performance on sensory-motor tasks following photothrombosis

To assess the functional impact of the photothrombotic lesions, we assessed animals prelesion to establish a baseline and again 24 h postlesion. We used two sensory-motor tasks that have been documented to demonstrate lesion severity: the rung walk (Farr et al., 2006) (Fig. 3A) and the adhesive dot removal test (Schallert and Whishaw, 1984) (Fig. 3C). Prelesion mice show very few errors during trials on the rung walk, with wild-type mice showing an average of 0.14 ± 0.06 errors/step and dnSNARE mice showing 0.15 ± 0.10 errors/step (Fig. 3B). In contrast, 24 h postlesion wild-type mice show a significant increase in the number of errors per step (12.41 ± 1.69) compared with prelesion ($p < 0.001$; Fig. 3B). dnSNARE mice also show a significant increase in the number of errors per step 24 h postlesion (7.57 ± 1.06 ; $p < 0.001$) compared with prelesion. However, compared with wild-type mice (12.41 ± 1.69), dnSNARE mice show significantly fewer errors postlesion (7.57 ± 1.06 ; $p = 0.002$; Fig. 3B).

In the adhesive dot removal test, prelesion animals were able to remove the adhesive dot in < 2 s (1.98 ± 0.30 s, wild-type; 2.03 ± 0.35 s, dnSNARE; Fig. 3D). At 24 h postlesion, wild-type mice take an average of 12.32 ± 1.90 s to remove the adhesive dot, while dnSNARE mice take an average of 7.34 ± 1.01 s, both of which are significantly increased compared with prelesion times ($p < 0.001$; Fig. 3B). Comparison of wild-type (12.32 ± 1.90 s) and dnSNARE (7.34 ± 1.01 s) postlesion reveals a significant difference ($p = 0.004$) in postlesion performance (Fig. 3B).

Involvement of an NMDA signaling pathway

It is well known that cerebral ischemia can trigger NMDA receptor-mediated excitotoxicity, and indeed NMDA lesions are used as a model of the excitotoxic component of ischemic damage (Meldrum and Garthwaite, 1990; Kim et al., 2006; Lipton, 2007). Because astrocytic dnSNARE expression leads to reduced neuronal NMDA receptor expression, we asked whether dnSNARE expression would be protective against NMDA-induced lesions. Mice were injected unilaterally with $1 \mu\text{l}$ of a 10 mg/ml solution of NMDA into the sensorimotor cortex, and 24 h later were killed and NMDA lesion volume was assessed (Fig. 4A). Mice expressing dnSNARE within astrocytes had a significantly reduced NMDA lesion volume ($0.131 \pm 0.0129 \text{ mm}^3$) compared with wild-type mice ($0.207 \pm 0.0260 \text{ mm}^3$; $p = 0.040$) as assessed by Nissl staining (Fig. 4A, C).

Tissue sections from mice that had undergone unilateral NMDA lesions were also processed for immunohistochemistry for NeuN (Fig. 4B). Within the NMDA lesion region, wild-type mice had an average of 0.96 ± 0.26 NeuN-positive neurons per $62,500 \mu\text{m}^3$ (± 0.26 ; Fig. 4D). In contrast, mice expressing dn-

photothrombosis infarct and peri-infarct regions in wild-type and dnSNARE mice. EGFP-positive astrocytes (green) are only visible in mice expressing dnSNARE. **B**, Representative image of NeuN staining in hemisphere contralateral to the photothrombosis infarct in wild-type and dnSNARE mice. **C**, Quantification of the number of NeuN-positive neurons per $62,500 \mu\text{m}^3$ in infarct, peri-infarct, and contralateral regions of wild-type and dnSNARE mice subjected to photothrombosis. I, Infarct; P, peri-infarct. * $p < 0.05$.

SNARE had an average of 5.50 ± 1.48 NeuN-positive neurons per $62,500 \mu\text{m}^3$, demonstrating that dnSNARE mice had significantly greater numbers of spared neurons within the NMDA lesion ($p = 0.024$; Fig. 4D). No difference was observed in the number of NeuN-positive neurons per $62,500 \mu\text{m}^3$ in cortical tissue contralateral to the NMDA lesion between wild-type littermate (14.83 ± 1.70) and dnSNARE (15.67 ± 1.33) mice.

Discussion

Astrocytes are well poised to impact the outcome of stroke because they are both structurally and functionally linked to both neurons and the vasculature (Haydon and Carmignoto, 2006; Attwell et al., 2010). From the data presented in this study, we propose that an astrocytic SNARE signaling pathway plays a key role in the extent of damage following ischemic insult. We report that dnSNARE animals have decreased infarct volume, and increased sparing of NeuN-positive neurons following photothrombotic damage in both the infarct and peri-infarct regions. We also observed a functional sparing in dnSNARE mice when animals that had undergone photothrombotic injury were tested 24 h after lesion induction. Using the rung walk task and the adhesive dot removal tests, we demonstrate that the sensorimotor areas have been functionally spared in the dnSNARE mice compared with wild-type mice receiving matched lesions.

There are many mechanisms that could mediate this protective effect. Previous studies using dnSNARE mice have shown that astrocytes regulate neuronal NMDA receptor trafficking. By releasing adenosine, astrocytes activate neuronal A1R that in turn stimulates an src family kinase-dependent regulation of NMDA receptor trafficking. When dnSNARE is expressed in astrocytes, this glial source of adenosine is lost, leading to a reduction in neuronal NMDA receptors (Deng et al., 2011). Consequently, we propose that the ability of astrocytic dnSNARE expression to be neuroprotective is mediated in part by the loss of neuronal NMDA receptors. In agreement with this possibility, we found that the magnitude of NMDA-induced lesions is reduced in dnSNARE mice.

In addition to effects mediated by reduced cell surface NMDA receptors is the possibility that a dnSNARE-dependent reduction in the Ca^{2+} -dependent release of D-serine from astrocytes leads to a reduction in NMDA receptor-mediated currents and thus to neuronal protection. For example, we have shown that dnSNARE mice exhibit reduced D-serine regulation of NMDA receptors: in dnSNARE mice, exogenous D-serine led to a greater augmentation of the NMDA receptor-mediated current than in wild-type littermates (Fellin et al., 2009). In support of this possibility, we have shown a significant reduction of infarct volume of 47% by decreasing astrocytic Ca^{2+} , suggesting that the increased astrocytic Ca^{2+} signals in astrocytes contribute to ischemic damage (Ding et al., 2009).

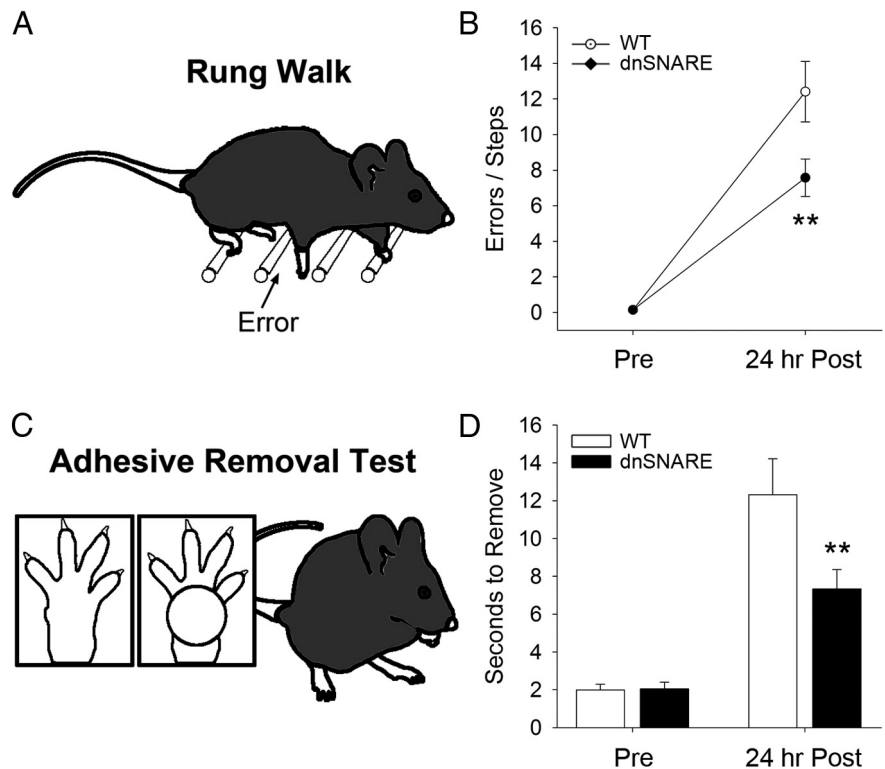


Figure 3. Mice expressing dnSNARE perform significantly better following photothrombosis on sensory-motor tasks compared with matched wild-type controls. **A**, Schematic of rung-walk task, which requires mice to walk along a horizontal ladder to a goal box. In this task, errors are counted when the mouse misses grasping the rung during a crossing, causing the paw to slip between two rungs. **B**, Quantification of the number of errors per step in wild-type and dnSNARE mice before photothrombosis, and again at 24 h of reperfusion. **C**, Schematic of the adhesive dot removal test, which requires mice to remove an adhesive dot from their forepaw. **D**, Quantification of the time required to remove the adhesive dot in wild-type and dnSNARE mice before photothrombosis, and at 24 h. $**p < 0.01$.

The changes observed by Ding et al. (2009) are particularly interesting because enhanced astrocytic calcium has been shown to induce the release of glutamate and D-serine, which interact with the NR2B subunit of NMDA receptors (Araque et al., 1998; Parpura and Haydon, 2000; Aguado et al., 2002; Angulo et al., 2004; Fellin et al., 2004). We have previously shown that following status epilepticus enhanced astrocytic Ca^{2+} signals could activate the neuronal NR2B subunit of NMDA receptors, resulting in delayed neuronal death (Ding et al., 2009).

Based on animal models of focal ischemia, numerous mechanisms of damage have been proposed, including glutamate-mediated exocytosis, oxidative stress, changes in pH and acidosis, and changes in mitochondrial function (Barber et al., 2003; Mattiasson et al., 2003; Xiong et al., 2004; Eltzschig and Eckle, 2011). In particular, the NMDA receptor has been shown to be critical for excitotoxicity following ischemia, and has been shown to increase intracellular Ca^{2+} levels and the initiation of both necrotic and apoptotic pathways (Szatkowski and Attwell, 1994; Martin et al., 1998; Aarts et al., 2003; Arundine and Tymianski, 2003, 2004). That a manipulation in the astrocytic dnSNARE signaling pathway can disrupt this process suggests that astrocytes impact cell loss that arises from ischemic injuries.

References

- Aarts MM, Arundine M, Tymianski M (2003) Novel concepts in excitotoxic neurodegeneration after stroke. *Expert Rev Mol Med* 5:1–22. [CrossRef Medline](#)
- Aguado F, Espinosa-Parrilla JF, Carmona MA, Soriano E (2002) Neuronal

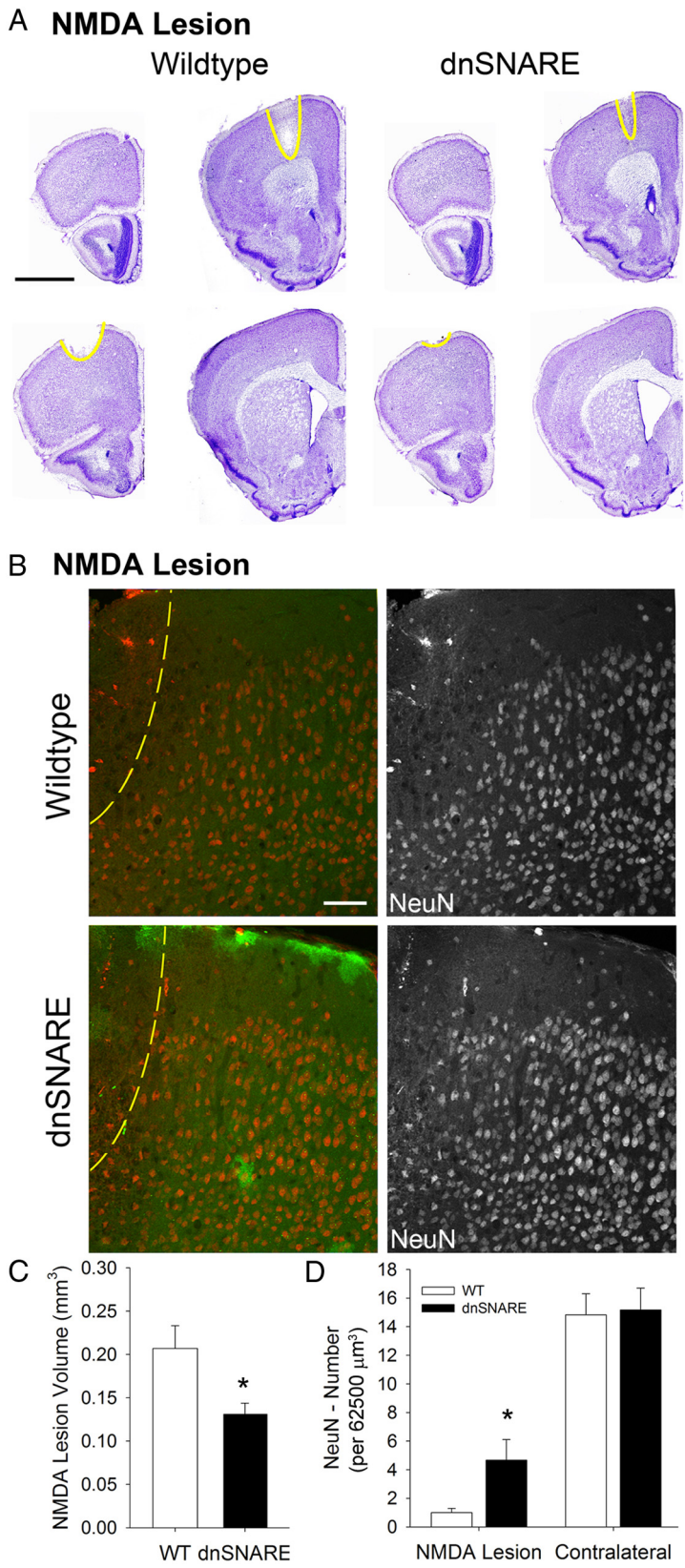


Figure 4. Damage following NMDA lesions is attenuated by dnSNARE expression in astrocytes. **A**, Representative images of Nissl-stained sections from wild-type and dnSNARE mice subjected to unilateral NMDA lesions. **B**, Representative image of NeuN (red) staining in wild-type and dnSNARE mice subjected to unilateral NMDA lesions. **C**, Quantification of NMDA lesion volume calculated from reconstructed Nissl-stained serial section sets in wild-type and dnSNARE mice. **D**, Quantification of the number of NeuN-positive neurons per 62,500 μm³ in wild-type and dnSNARE mice in NMDA lesion and contralateral cortical tissue. **p* < 0.05.

activity regulates correlated network properties of spontaneous calcium transients in astrocytes *in situ*. *J Neurosci* 22:9430–9444. Medline

Angulo MC, Kozlov AS, Charpak S, Audinat E (2004) Glutamate released from glial cells synchronizes neuronal activity in the hippocampus. *J Neurosci* 24:6920–6927. CrossRef Medline

Araque A, Sanzgiri RP, Parpura V, Haydon PG (1998) Calcium elevation in astrocytes causes an NMDA receptor-dependent increase in the frequency of miniature synaptic currents in cultured hippocampal neurons. *J Neurosci* 18:6822–6829. Medline

Arundine M, Tymianski M (2003) Molecular mechanisms of calcium-dependent neurodegeneration in excitotoxicity. *Cell Calcium* 34:325–337. CrossRef Medline

Arundine M, Tymianski M (2004) Molecular mechanisms of glutamate-dependent neurodegeneration in ischemia and traumatic brain injury. *Cell Mol Life Sci* 61:657–668. CrossRef Medline

Attwell D, Buchan AM, Charpak S, Lauritzen M, Macvicar BA, Newman EA (2010) Glial and neuronal control of brain blood flow. *Nature* 468:232–243. CrossRef Medline

Barber PA, Demchuk AM, Hirt L, Buchan AM (2003) Biochemistry of ischemic stroke. *Adv Neurol* 92:151–164. Medline

Barreto G, White RE, Ouyang Y, Xu L, Giffard RG (2011a) Astrocytes: targets for neuroprotection in stroke. *Cent Nerv Syst Agents Med Chem* 11:164–173. CrossRef Medline

Barreto GE, Gonzalez J, Torres Y, Morales L (2011b) Astrocytic-neuronal crosstalk: implications for neuroprotection from brain injury. *Neurosci Res* 71:107–113. CrossRef Medline

Brown CE, Boyd JD, Murphy TH (2010) Longitudinal *in vivo* imaging reveals balanced and branch-specific remodeling of mature cortical pyramidal dendritic arbors after stroke. *J Cereb Blood Flow Metab* 30:783–791. CrossRef Medline

Deng Q, Terunuma M, Fellin T, Moss SJ, Haydon PG (2011) Astrocytic activation of A1 receptors regulates the surface expression of NMDA receptors through a Src kinase dependent pathway. *Glia* 59:1084–1093. CrossRef Medline

Ding S, Wang T, Cui W, Haydon PG (2009) Photostimulation of ischemia stimulates a sustained astrocytic Ca²⁺ signaling *in vivo*. *Glia* 57:767–776. CrossRef Medline

Eltzschig HK, Eckle T (2011) Ischemia and reperfusion—from mechanism to translation. *Nat Med* 17:1391–1401. CrossRef Medline

Farr TD, Liu L, Colwell KL, Whishaw IQ, Metz GA (2006) Bilateral alteration in stepping pattern after unilateral motor cortex injury: a new test strategy for analysis of skilled limb movements in neurological mouse models. *J Neurosci Methods* 153:104–113. CrossRef Medline

Fellin T, Pascual O, Gobbo S, Pozzan T, Haydon PG, Carmignoto G (2004) Neuronal synchrony mediated by astrocytic glutamate through activation of extrasynaptic NMDA receptors. *Neuron* 43:729–743. CrossRef Medline

Fellin T, Halassa MM, Terunuma M, Succol F, Ta-

- kano H, Frank M, Moss SJ, Haydon PG (2009) Endogenous nonneuronal modulators of synaptic transmission control cortical slow oscillations in vivo. *Proc Natl Acad Sci U S A* 106:15037–15042. [CrossRef Medline](#)
- Ginsberg MD, Pulsinelli WA (1994) The ischemic penumbra, injury thresholds, and the therapeutic window for acute stroke. *Ann Neurol* 36:553–554. [CrossRef Medline](#)
- Halassa MM, Florian C, Fellin T, Munoz JR, Lee SY, Abel T, Haydon PG, Frank MG (2009) Astrocytic modulation of sleep homeostasis and cognitive consequences of sleep loss. *Neuron* 61:213–219. [CrossRef Medline](#)
- Haydon PG (2001) GLIA: listening and talking to the synapse. *Nat Rev Neurosci* 2:185–193. [CrossRef Medline](#)
- Haydon PG, Carmignoto G (2006) Astrocyte control of synaptic transmission and neurovascular coupling. *Physiol Rev* 86:1009–1031. [CrossRef Medline](#)
- Hossmann KA (1994) Viability thresholds and the penumbra of focal ischemia. *Ann Neurol* 36:557–565. [CrossRef Medline](#)
- Hoyte L, Barber PA, Buchan AM, Hill MD (2004) The rise and fall of NMDA antagonists for ischemic stroke. *Curr Mol Med* 4:131–136. [CrossRef Medline](#)
- Ikonomidou C, Turski L (2002) Why did NMDA receptor antagonists fail clinical trials for stroke and traumatic brain injury? *Lancet Neurol* 1:383–386. [CrossRef Medline](#)
- Kim SH, Won SJ, Mao XO, Jin K, Greenberg DA (2006) Molecular mechanisms of cannabinoid protection from neuronal excitotoxicity. *Mol Pharmacol* 69:691–696. [Medline](#)
- Lipton SA (2004) Failures and successes of NMDA receptor antagonists: molecular basis for the use of open-channel blockers like memantine in the treatment of acute and chronic neurologic insults. *NeuroRx* 1:101–110. [CrossRef Medline](#)
- Lipton SA (2007) Pathologically-activated therapeutics for neuroprotection: mechanism of NMDA receptor block by memantine and S-nitrosylation. *Curr Drug Targets* 8:621–632. [CrossRef Medline](#)
- Martin LJ, Al-Abdulla NA, Brambrink AM, Kirsch JR, Sieber FE, Portera-Cailliau C (1998) Neurodegeneration in excitotoxicity, global cerebral ischemia, and target deprivation: a perspective on the contributions of apoptosis and necrosis. *Brain Res Bull* 46:281–309. [CrossRef Medline](#)
- Mattiasson G, Shamloo M, Gido G, Mathi K, Tomasevic G, Yi S, Warden CH, Castilho RF, Melcher T, Gonzalez-Zulueta M, Nikolich K, Wieloch T (2003) Uncoupling protein-2 prevents neuronal death and diminishes brain dysfunction after stroke and brain trauma. *Nat Med* 9:1062–1068. [CrossRef Medline](#)
- Meldrum B, Garthwaite J (1990) Excitatory amino acid neurotoxicity and neurodegenerative disease. *Trends Pharmacol Sci* 11:379–387. [CrossRef Medline](#)
- Muir KW (2006) Glutamate-based therapeutic approaches: clinical trials with NMDA antagonists. *Curr Opin Pharmacol* 6:53–60. [CrossRef Medline](#)
- Oliet SH, Piet R, Poulain DA, Theodosis DT (2004) Glial modulation of synaptic transmission: insights from the supraoptic nucleus of the hypothalamus. *Glia* 47:258–267. [CrossRef Medline](#)
- Parpura V, Haydon PG (2000) Physiological astrocytic calcium levels stimulate glutamate release to modulate adjacent neurons. *Proc Natl Acad Sci U S A* 97:8629–8634. [CrossRef Medline](#)
- Pascual O, Casper KB, Kubera C, Zhang J, Revilla-Sanchez R, Sul JY, Takano H, Moss SJ, McCarthy K, Haydon PG (2005) Astrocytic purinergic signaling coordinates synaptic networks. *Science* 310:113–116. [CrossRef Medline](#)
- Schallert T, Whishaw IQ (1984) Bilateral cutaneous stimulation of the somatosensory system in hemidecorticate rats. *Behav Neurosci* 98:518–540. [CrossRef Medline](#)
- Szatkowski M, Attwell D (1994) Triggering and execution of neuronal death in brain ischaemia: two phases of glutamate release by different mechanisms. *Trends Neurosci* 17:359–365. [CrossRef Medline](#)
- Tennant KA, Adkins DL, Donlan NA, Asay AL, Thomas N, Kleim JA, Jones TA (2011) The organization of the forelimb representation of the C57BL/6 mouse motor cortex as defined by intracortical microstimulation and cytoarchitecture. *Cereb Cortex* 21:865–876. [CrossRef Medline](#)
- Watson BD, Dietrich WD, Busto R, Wachtel MS, Ginsberg MD (1985) Induction of reproducible brain infarction by photochemically initiated thrombosis. *Ann Neurol* 17:497–504. [CrossRef Medline](#)
- Xiong ZG, Zhu XM, Chu XP, Minami M, Hey J, Wei WL, MacDonald JF, Wemmie JA, Price MP, Welsh MJ, Simon RP (2004) Neuroprotection in ischemia: blocking calcium-permeable acid-sensing ion channels. *Cell* 118:687–698. [CrossRef Medline](#)
- Zorec R, Araque A, Carmignoto G, Haydon PG, Verkhratsky A, Parpura V (2012) Astroglial excitability and gliotransmission: an appraisal of Ca²⁺ as a signalling route. *ASN Neuro* 4:e00080. [CrossRef Medline](#)